A miniature frequency-stabilized VCSEL system emitting at 795 nm based on LTCC modules

Florian Gruet[1], Fabrizio Vecchio[2], Christoph Affolderbach[1], Yves Pétremand[3], Nico F. de Rooij[3], Thomas Maeder[2], Gaetano Mileti[1]

[1] Laboratoire Temps-Fréquence (LTF), Institut de Physique, Université de Neuchâtel, Avenue de Bellevaux 51, 2000 Neuchâtel, Switzerland.

[2] Laboratoire de Production Microtechnique (LPM2), Ecole Polytechnique Fédérale de Lausanne (EPFL), EPFL STI IMT LPM2, Station 17, 1015 Lausanne, Switzerland.

[3] Sensors, Actuators and Microsystems Laboratory (SAMLAB), Institute of Microtechnology (IMT), Ecole Polytechnique Fédérale de Lausanne (EPFL), Jaquet-Droz 1, 2000 Neuchâtel, Switzerland

Abstract

We present a compact frequency-stabilized laser system locked to the Rubidium absorption line of a micro-fabricated reference cell. A Printed Circuit Board (PCB) is used to carry all the components and part of the electronics, and Low-Temperature Co-fired Ceramic (LTCC) modules are used to temperature-stabilize the laser diode and the miniature Rubidium cell (cell inner dimensions: 5 mm diameter and 2 mm height). The measured frequency stability of the laser, in terms of Allan deviation, is $\leq 8\times10^{-10}$ for integration times of $10^3 - 10^5$ seconds. The current overall dimensions of the system are 70 × 40 × 50 mm^3, with good potential for realization of a frequency-stabilized laser module with few cm^3 volume.

1. Introduction

Laser sources with accurate frequency stability are widely used and necessary in many applications, such as interferometric detection, spectroscopy [1], optical communications and atomic magnetometers [2] and clocks [3]. Moreover, they are also used in commercial applications such as precision machining tools, laser vibrometers [4] and gravimeters [5]. In such applications, on the one hand, there is the need of reducing the power consumption and the dimensions of the laser source, in order to facilitate the fabrication of portable devices; on the other hand, the demand for highly-stable laser sources is rapidly increasing, with the ever more widespread diffusion of applications based on, e.g. high-resolution spectroscopy [1] or precise navigation systems using atomic clocks [6]. In this context, the objective of this research is to design and fabricate a compact and low-power frequency-stabilized laser, in particular for use in miniature atomic clocks [3]. Similar spectroscopy modules with high compactness have been previously developed [7], but no frequency stability of the system was reported.

To achieve this objective, low-temperature-co-fired-ceramic (LTCC) technology was used to integrate temperature sensor and control in a compact module; a micro-fabricated Rb vapor cell was used to precisely stabilize the frequency of a vertical-cavity-surface-emitting-laser (VCSEL) [8] to a Doppler-broadened absorption resonance of the ^{85}Rb D1 line. The designed system presents the following advantages:

- VCSELs are very cost-efficient and low-power consumption laser sources.
- The use of LTCC technology allows integrating temperature measurement and heating in one small module, reducing the size of the device and also limiting the dissipated power.

- The use of Rb cell as a frequency reference gives good long-term stability, thanks to the intrinsic stability of the Rb atomic reference. These Rb absorption lines show small frequency shifts in response to external factors such as magnetic fields or temperature changes.
- Micro-fabrication of the Rb cell allows a very compact realization.

2. Design and fabrication of the system

The main optical components of the system are the VCSEL laser diode, the reference Rb cell and the photo-detector. The VCSEL laser diode and the reference cell are both glued using a thin layer of thermally conductive silicone adhesive (Q5-8401 Dow Corning) onto a low-temperature co-fired ceramic (LTCC) platform, which provides the temperature control for the components. A commercial photo-detector is glued on a simple support PCB. The resulting three modules are mounted vertically, together with a beamsplitter, on a PCB which acts as a carrier for the whole system and provides the analog conditioning electronics for temperature measurement. Fig. 1 shows a 3D block diagram of the system:

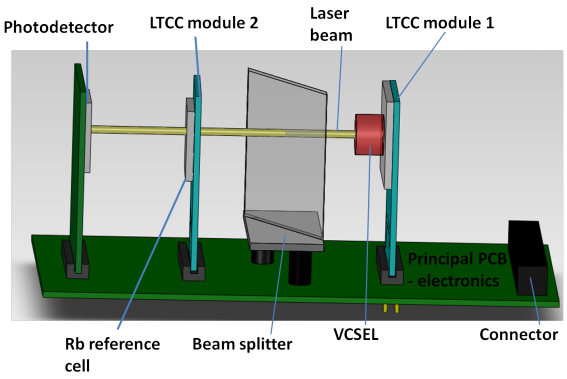

Fig.1. 3D block diagram of the system.

1.1 LTCC module fabrication and description

An LTCC module equipped with a heating serpentine and a positive temperature coefficient (PTC) resistor for temperature measurement was fabricated and used to temperature-stabilize the VCSEL and the reference cell. The fabrication process of the LTCC module involves the standard steps of this technology [9]: design of the circuit, laser cutting of green tapes, screen-printing, stacking and lamination, and firing. The final device is 500 µm thick and it is composed of 4 layers. Several additional intermediate empty layers could be added, depending on thickness requirements. A thicker module is more robust and able to carry heavier weight, but it demands a longer, more expensive fabrication process and entails a higher thermal conductivity loss.

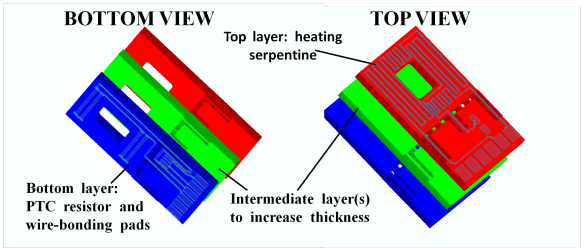

Fig.2. Schematic of the LTCC module designed.

The fabrication of this particular LTCC device has been described in [10]. The use of two different LTCC green tapes (nominal 0 x-y shrinkage HL 2000 from Heraeus, Germany and DP951 from DuPont, USA) allowed obtaining almost zero shrinkage (precisely, x shrinkage of the module was 1.079% and y shrinkage was 0.844%), without having to stack many thin HL layers. The conductive AgPd paste used to screen-print the connection tracks, the solder pads and the heating serpentine was DuPont (DP)6146. Finally, the PTC resistor paste DuPont (DP) 5092D was used to screen-print the PTC temperature sensor, which was calibrated before use. The overall dimensions of the LTCC module are 15×22 mm^2; there is an aperture at the center of dimensions 5×5 mm^2 for mounting the cell and the VCSEL, and the total heated area is 15×12 mm^2. This heated area is insulated from the external "cold" area, where the electrical connections are placed: both zones only communicate through two small bridges (Figs. 2 and 3) of dimensions 0.6×5 mm^2. Another additional optional central bridge is present in the original configuration. This bridge can be cut away if low-loss configuration is desired (Fig. 3a), or kept, if a more robust module able to withstand heavier weight is preferred (Fig. 3b). When equipped with the

intermediate bridge, a controlled temperature gradient is introduced into the system in the form of an additional conduction loss, which thermal simulations show to be approx. 20% with respect to the low-loss configuration [11]. Moreover, it is possible to further adjust the temperature gradient between two well-defined regions of the heated area using an SMD resistor, soldered on dedicated pads (Fig.3b), which changes the current flow in the bottom part of the heated area. The resulting colder zone is useful for introducing a well-defined "cold point" in the Rb reference cells, which helps avoiding unwanted formation of alkali metal droplets on the cell windows. Simulations show that the LTCC heater, when no losses are present into the system other than conduction in the LTCC bridges (complete vacuum, no radiation) is able to get a temperature of 70°C at the hot zone with a minimum heating power of 31 mW (3.25 V, 9.6 mA).

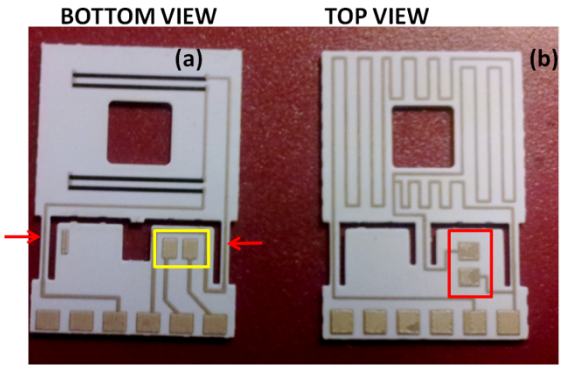

Fig.3. A photo of the fabricated LTCC module: (a) bottom view, module without optional central bridge. The PTC resistor consists of the four black lines on the top part. The red arrows highlight the two small bridges that connect the cold zone (bottom) and the hot zone (top). In the yellow rectangle there are the wire-bonding pads. (b) Top), top view of the module, with optional central bridge. The heating silver serpentine covers the entire hot zone on the top. In the red rectangle there are SMD pads where it is possible to solder a resistor that will alter the current flow through the bottom part of the heated area.

Moreover, in case the bottom part of the serpentine is disabled (short circuit on the dedicated solder pads), simulations show that the unheated zone is 10°C colder than the heated area, when the latter is kept at 70°C and in case the module is efficiently thermally insulated [11]. On the bottom layer, there are also wire-bonding pads (Fig. 3a), in case additional devices (e.g. external sensors) must be added and connected to the carrier PCB.

2.2 Miniature reference cell

The reference cell is fabricated using micro-fabrication techniques. The first fabrication steps are carried out at wafer level and the last ones at chip level.

First, a preform is built by bonding anodically a borofloat wafer with a 2 mm-thick silicon wafer containing cavities etched through. These cavities are etched in the silicon wafer by deep reactive ion etching (DRIE) and are defined by a photoresist and silicon dioxide mask. The wafer is then diced into 10 × 10 mm^2 chips.

The second part of the process is performed at chip level. The diced preforms obtained are cleaned and prepared to be placed into a dedicated machine allowing dispensing alkali metal inside the cell cavity and closing it by bonding anodically a glass lid on top [12]. Before sealing the cell, a controlled pressure of gas mixture can be inserted into the machine and inside the cell cavity.

For the application example of a miniature atomic clock, the micro-fabricated Rb cell usually contains around 100 mbar of an inert buffer gas [3]. In order to obtain results representative for such type of applications from this study, a micro-fabricated Rb cell containing 60 mbar of an Ar–Ne mixture as a buffer gas was fabricated and used for this study.

2.3 Principal PCB – assembling of the system

A horizontal PCB acts as a carrier for the whole system and also carries the required electronics for temperature measurement (Wheatstone

bridge using the PTC on the LTCC module as sensitive element coupled with a first pre-amplification of the temperature signal) and trans-impedance amplifier for the photo-detector. Standard DIN connectors are used to connect the various modules vertically (see the block diagram in Fig. 1). The total dimensions of the PCB are currently 70 × 40 mm^2. A photo of the assembled system is shown in Fig. 4, which can be compared with the block diagram in Fig. 1.

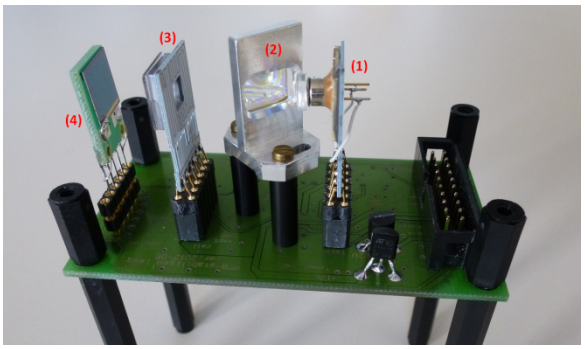

Fig.4. Picture of the assembled system with: (1) laser; (2) beamsplitter; (3) Rb cell; (4) detector.

3. Frequency stability measurements

The Doppler-broadened Rb absorption signal of the micro-fabricated Rb cell is used to lock the laser, which is a much simpler approach than saturated-absorption spectroscopy [6] and more compact than previous studies using a thin cesium cell [13,14]. In our case, the Doppler lines are further broadened due to collisions between the Rb atoms and the buffer gas, which corresponds to the practical case encountered for miniature atomic clocks [3]. In order to increase the absorption signal, the cell is heated up to approximately 100°C by the LTCC module. The laser can be frequency-stabilized to either ^{85}Rb or ^{87}Rb absorption lines. Fig. 6 shows the Doppler-broadened absorption spectrum, obtained with a laser injection current of 2 mA and a laser temperature of 49°C. The cell is heated to 95°C and the laser optical power through the cell is about 45 µW.

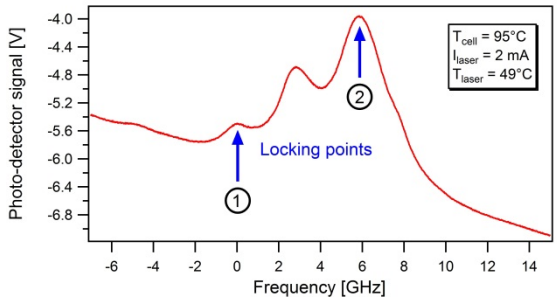

Fig.5. Doppler-broadened absorption spectrum. The peak labeled 1 corresponds to ^{87}Rb and the peak labeled 2 corresponds to the ^{85}Rb.

Laser frequency stabilization is achieved by frequency-modulation of the VCSEL output (via its injection current) and subsequent lock-in detection of the absorption signal. The derived correction signal is applied to the VCSEL injection current.

3.1 Experimental setup

The frequency stability measurements have been performed by beat-note between the laser system and a reference Laser Head that has a frequency stability of 2.4 × 10^{-11} at 1 s and < 1 × 10-^{10} at all timescale up to 1 day [15]. A beamsplitter has been implemented on the laser system in order to send a part of the beam to an optical fiber, superimposed with the beam of the Laser Head. Even if the two lasers are stabilized to the same atomic transition (in the case of ^{87}Rb), the beat frequency can be measured thanks to the fact that the cell of the Laser Head contains pure ^{87}Rb only (without buffer gas) and the micro-fabricated cell of the laser system contains buffer gas in addition to Rb atoms. This addition of buffer gas broadens the absorption spectrum but also shift the atomic transition frequency by a few hundreds of MHz, resulting in a beat frequency around 325 MHz and 530 MHz when stabilizing to pointspoint 1 and 2 in Fig.5, respectively. This beat frequency is detected by a fast photo-detector and measured by a frequency counter referenced to an active hydrogen maser serving as a frequency reference. The setup is shown in Fig. 6.

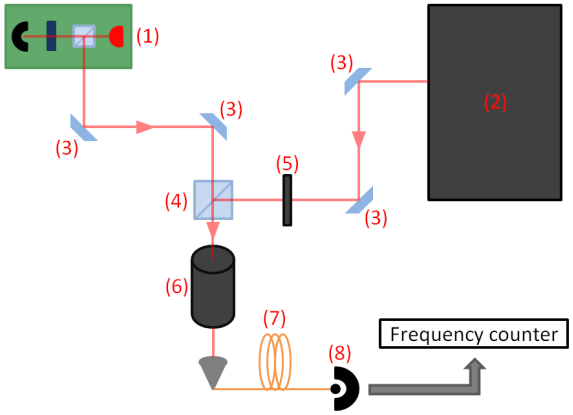

Fig. 6. Schematics of the measurement setup with: (1) laser system; (2) reference laser head; (3) mirrors; (4) non-polarizing beamsplitter cube; (5) λ/2 waveplate; (6) optical isolator; (7) single-mode optical fiber; (8) fast photo-detector.

The measurement of the beat allows searching for optimized operation parameters, such as the cell temperature and the laser optical power through the cell, that minimize the sensitivity of the stabilized laser frequency to variations in these system parameters. By recording the beat frequency with the laser frequency-stabilized to the ^{85}Rb line (point 2, Fig. 5), for different cell temperature and different light power through the cell, operating points with the smallest sensitivity to these parameters could be found, as shown in Fig. 7 and 8. A cell temperature of 104°C and a light power through the cell of 40 µW are identified as best operation parameters for optimized frequency stability.

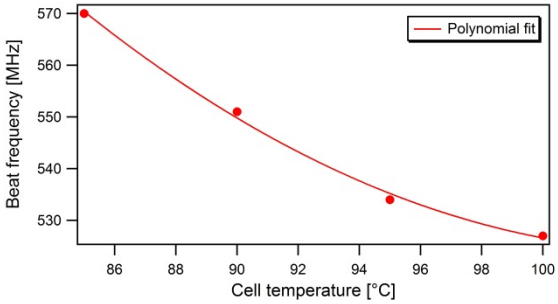

Fig.7. Beat frequency vs. cell temperature.

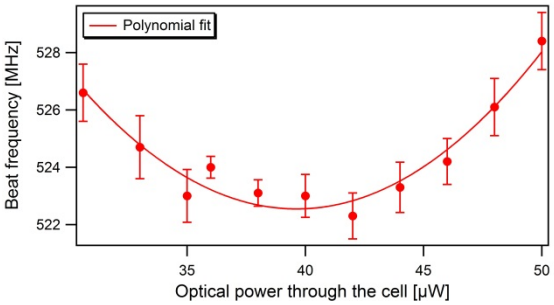

Fig.8. Beat frequency vs. optical power through the cell.

4. Results and discussion

Best laser frequency stability was obtained with the laser stabilized to the ^{85}Rb line (point 2, fig.5) resulting in a fractional frequency stability of 1.3×10^{-10} at 1 s and $\leq 8 \times 10^{-10}$ for all timescales up to 1 day (see Fig. 9). For stabilization to the ^{87}Rb line, a frequency stability of $3 \times 10\text{-}^{10}$ at 1 s is obtained. This difference is due to the fact that the signal-to-noise-ratio of the absorption signal is higher for the ^{85}Rb line than for the ^{87}Rb line (point 1, Fig. 5). However, for a laser to be frequency-stabilized to ^{87}Rb, the frequency stability could be improved by using an enriched ^{87}Rb micro-fabricated cell.

We can compare the frequency stability at 1 s obtained for the two conditions (^{85}Rb and ^{87}Rb) with their respective theoretical estimations by using the following equation:

$$\sigma_{th}(\tau) = \frac{N_{PSD}}{\sqrt{2} \cdot \nu_{laser} \cdot D} \cdot \tau^{-1/2} \qquad (1)$$

with N_{PSD} the power spectral density noise of the absorption signal, ν_{laser} the VCSEL's frequency and D the discriminator slope in the error signal, obtained from the absorption signal [16]. With the values given in Table 1, we calculated a frequency stability limit at 1 s of 7.2×10^{-11} and 1.3×10^{-10} for laser stabilization to ^{85}Rb and ^{87}Rb, respectively. The measured stability fits well with these estimated stability limits, within a factor of two.

Parameter	Units	^{85}Rb	^{87}Rb
Discriminator slope	V/GHz	0.35	1.67
PSD Noise	$V_{rms}/\sqrt{Hz}$	1.3×10^{-5}	1.2×10^{-4}
Estimated stability	$\tau^{-1/2}$	7.2×10^{-11}	1.3×10^{-10}
Measured stability	$\tau^{-1/2}$	1.3×10^{-10}	3×10^{-10}

Table 1: Short-term frequency stability estimation in accordance with equation (1), and experimentally measured result.

It is also important to notice that the stability measurements are not limited by the reference laser head, which has a frequency stability below 1×10^{-10} at all timescales of relevance here [15]. If we consider that the long-term stability (at $\tau > 10^3$ s) is limited by the temperature variations of the micro-fabricated Rb cell here, and referring to the results obtained in Fig.7, this would mean that the cell temperature varies of 0.1 K over 1one day. This might be possible considering the fact that the cell currently is heated on one side only, and is not perfectly thermally isolated, so temperature gradients across the cell may be present. Assuming an improved control of the cell temperature to the 10 mK level in a future realization, the long-term stability limit for the laser frequency may be reduced to around 5×10^{-11}. From a sensitivity of < 200 kHz/mW with respect to laser power (estimated from Fig. 8) and a stability of the laser power on the level of 1% over 1 day, laser power instabilities are estimated to contribute a frequency instability on the level of $\approx 2 \times 10^{-10}$ at 1 day, which is not limiting the experimental results of Fig. 9. For a further optimized thermal design (temperature stability improved by a factor of 10), our laser system is therefore expected to be compatible with a laser frequency stability on the level of $\approx 2 \times 10^{-10}$ at 1 day.

The dissipated power for the heating of the laser and the cell has been measured to be 75 mW and 920 mW, respectively. These results were obtained at room temperature with the laser heated at 48°C and the cell at 104°C, which are the optimum settings for the stability measurements. Thus, the assembled laser system shows low heating power consumption with less than 1 W for the laser and the cell. This dissipation can be further reduced by improving on the system's thermal isolation.

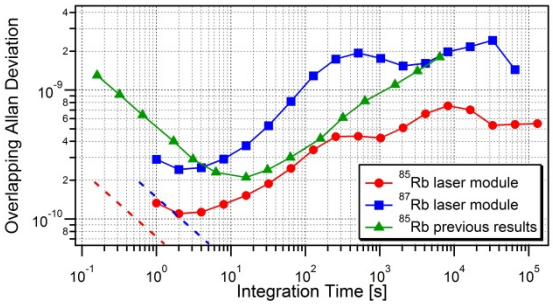

Fig.9: Frequency stability in terms of Allan deviation for ^{85}Rb (red dots), ^{87}Rb (blue squares) and previous results obtained with a bigger setup on ^{85}Rb (green triangles, [16]). The estimated S/N limits are the red and blue dashed lines.

5. Conclusions

We have presented the realization of a VCSEL laser system frequency-stabilized to a micro-fabricated Rb reference cell containing a considerable amount of buffer gas, as required for applications in e.g. miniature atomic clocks. Temperature control of both the Rb cell and the VCSEL laser was realized using custom-designed LTCC heater modules. The frequency stability of the system was measured by beat-note with a reference Laser Head, yielding a frequency stability of 1.3×10^{-10} at 1 s and $\leq 8 \times 10^{-10}$ up to 1 day for ^{85}Rb. This result is up to a factor of four better, depending on the timescale, than previously reported results obtained with a significantly bigger setup [16]. The main limiting factor for the measured frequency stability is currently due to residual temperature instabilities of the Rb reference cell. For a laser system with further improved temperature control of the micro-fabricated Rb cell, a laser frequency stability of around 2×10^{-10} at 1 day is expected.

Acknowledgements

This work was supported by the Swiss National Science Foundation, Sinergia Grant CRSI20_122693. We thank M. Pellaton and M. Dürrenberger (both LTF-UniNe) for valuable discussions and experimental support. We also thank M. Farine (LPM-Lausanne) for the effort produced in fabricating the LTCC modules.

References

[1] Schilt S, Tittel FK, Petrov KP, *Diode* laser spectroscopic monitoring *of* trace gases, Encyclopedia of analytical chemistry. John Wiley & Sons, Chichester; 2011.

[2] Budker D, Romalis M. Optical magnetometry. Nat Phys, 2007; 3:227.34.

[3] Knappe S. MEMS Atomic Clocks. Compr Microsyst 2007;3:571–612.

[4] Roos PA, Stephens M, Wieman CE. Laser vibrometer based on optical-feedback-induced frequency modulation of a single-mode laser diode. Appl Opt 1996;35:6754–61.

[5] Arnautov GP, et al. Gabl, an absolute free-fall laser gravimeter. Metrologia 1983;19:49–55.

[6] Bandi T, Affolderbach C, Calosso CE, Mileti G. High-performance laser-pumped rubidium frequency standard for satellite navigation. Electron Lett 2011;47:698–9.

[7] Knappe S, Robinson H, Hollberg L. Microfabricated saturated absorption laser spectrometer. Opt Exp 2007;15(10) May.

[8] Michalzik R, editor. VCSELs: fundamentals, technology and applications of vertical-cavity surface-emitting lasers, Springer series in optical sciences, vol. 166. Heidelberg & New York: Springer; 2013.

[9] Imanaka Y. Multilayered low temperature cofired ceramics (LTCC) technology. New York, NY: Springer; 2005 p. 142–90.

[10] V. Venkatraman, H. Shea, F. Vecchio, T. Maeder, P. Ryser, LTCC integrated miniature Rb discharge lamp module for stable optical pumping in miniature atomic clocks and magnetometers. In: Proceedings of IEEE 18th international symposium for design and technology in electronic packaging (SIITME); 2012.

[11] Vecchio F, Slater C, Maeder T, Ryser P. Thermal characterization of an LTCC module for miniature atomic clock packaging. CICMT 2012:484–91.

[12] Pétremand Y, Affolderbach C, Straessle R, Pellaton M, Briand D, Mileti G, et al. Microfabricated rubidium vapour cell with a thick glass core for small-scale atomic clock applications. J Micromech Microeng 2012;22:025013.

[13] Fukuda K, Furukawa M, Hayashi S, Tachikawa M. Frequency stabilization of a diode laser with a thin CS-vapor cell. IEEE Trans Ultrason Ferroelectr Freq Control 2000;47(2):502–5.

[14] Fukuda K, Tachikawa M, Kinoshita M. Allan-variance measurements of diode laser frequency-stabilized with a thin vapor cell. Appl Phys B 2003;77:823–7.

[15] F. Gruet, M. Pellaton, C. Affolderbach, T. Bandi, R. Matthey, G. Mileti, Compact and frequency stabilized laser heads for rubidium atomic clocks. In: Proceedings of international conference on space optics (ICSO), 2012.

[16] Di Francesco J, Gruet F, Schori C, Affolderbach C, Matthey R, Mileti G. Evaluation of the frequency stability of a VCSEL locked to a microfabricated Rubidium vapour cell. Proc SPIE 2010;7720:77201T.